International Journal of
Automotive Manufacturing and Materials（IJAMM）

Scilight

Article

Experimental Investigation of Gaseous Emissions and Hydrocarbon Speciation for MF and MTHF Gasoline Blends in DISI Engine

Rafiu K. Olalere [1,2], Gengxin Zhang [1], and Hongming Xu [1,3,*]

[1] Department of Mechanical Engineering, School of Engineering, University of Birmingham, Edgbaston, Birmingham B15 2TT, UK
[2] Department Mechanical Engineering, Lagos State University of Science and Technology, Ikorodu 02341, Nigeria
[3] State Key Laboratory of Automotive Safety and Energy, Tsinghua University, Beijing 100084, China
* Correspondence: h.m.xu@bham.ac.uk
Received: 08 November 2023; Revised: 18 February 2023; Accepted: 25 March 2024; Published: 28 March 2024

Abstract: With the increasing shortage of fossil energy, the development of engines urgently requires alternative fuels. Gaseous emissions of a gasoline direct injection spark ignition engine fueled with blends of 2-methylfuran (MF 20% vol. and gasoline 80% vol.) and 2-methyltetrahydrofuran (MTHF 20% vol. and gasoline 80% vol.) were experimentally investigated using Gasmeth FTIR. Experiments were conducted at air-fuel ratio (λ = 1) and at engine speed of 1500 rpm using the fuels optimised spark timing. Effects of fuel injection sweeps (180–280 °CA BTDC**)** on the emission characteristics of blends were investigated at the intermediate load of 5.5 bar IMEP. Hydrocarbon emission (HC) for gasoline is about 41% and 16% higher compared to MF20 and MTHF20 respectively. Carbon monoxide emission for the fuels increases as the injection timing is retarded but the Nitrogen oxide (NO_x) emissions was observed to reduce with the retarded injection timing. Both MF20 and MTHF20 recorded high NO_x emissions compared to gasoline. The results indicated ethylene (25–26%) as the major component of the HC speciation in the fuels investigated. The unburnt furan samples for blend fuels were determined to be less than 3% of HC emissions, which could be considered a safe level for exposure.

Keywords: 2-methylfuran (MF); 2-methyltetrahydrofuran (MTHF); un-leaded gasoline (ULG); direct-injection spark ignition (DISI); hydrocarbon speciation

1. Introduction

After 2010s, fuel researchers shifted focused to furan-based fuels as alternative engine fuels due to the breakthrough recorded in its method of production, which were reported by the Nature and Science [1–3]. Dumesic, Román, and Zhao have independently developed a highly efficient approach of converting fructose into furan-based fuels [4–6]. Ethanol that is hitherto premium as a renewable engine fuels suffers from several limitations, including high water solubility, high volatility and low energy density [7–9]. This is the motivation for the extensive research on furan fuels as a substitute to ethanol as alternative engine fuel. It was established that 2-methylfuran (MF) and 2-methylfurantetrahydrofuran (MTHF) have some properties that are more favourable for SI engines compares to ethanol.

MF has a low water solubility, which makes its gasoline blend more stable. The heat of vaporization of MF is low (358.4 kJ/kg) compared to gasoline (373 kJ/kg) [10, 11]. The volumetric energy density of MF (913.2 kg/m^3) is almost 23% higher than gasoline (744.6 kg/m^3) [1,12–14]. Most significantly, MF can avoid the engine cold-start problem than Ethanol due to its higher combustion stabilities and higher rates of vaporization. The in-cylinder spray formation and evaporation process indicates quicker evaporation of MF compared to ethanol [14]. Thewes et. al, reported that MF has a better knock resistance and higher

compression ratio than gasoline at full load leading to recorded efficiency improvements of up to 9.9% [8]. The hydrocarbon emissions (HC) from MF are at least 61% lower than gasoline [15,16]. In an investigation by Wang et. al on the Impacts of low-Level 2-methyl furan contents in gasoline, the low blend of MF consistently has lower HC emissions than gasoline. It was reported that Fuels such as MF with oxygenated molecules produce lower HC emissions due to the availability of more oxygen for combustion [15]. Nitrogen dioxides emissions (NO_x) and Carbon monoxide emissions (CO) emissions level of low blends of MF was found to increases with load because of the increasing combustion flame temperature [17]. Haigio et.al found that for low blends of MF variation of NO_x emissions with engine speeds increases exponentially with in-cylinder combustion temperature. It was however, reported that the NO_x emission by the low blends of ethanol was significantly low due to the cooling effect of ethanol which is the major merit of ethanol over the furan based fuels [18]. Pan et. al has used low Exhaust Gas Recirculation (EGR) rate conditions to solve the problem of high NO_x emissions from the combustion of MF. A significant downward trend in NO_x emissions was observed most especially after introducing appropriate EGR rates [14]. Gasoline and Ethanol has lower CO emissions compares to MF. The CO emissions are significantly influence by fuel/air equivalence ratio [15,19].

2-methyltetrahydrofuran is a component of P-series fuels. Analysts do not actually expect P-series fuels to replace gasoline, but its sales were expected to grow rapidly in the next 10 years [20]. Motivation for the use of MTHF as engine fuel is in its low cost of production. It can be produced from waste cellulose at a cost as low as US$ 0.60 per gallon [6]. MTHF-gasoline blends in a spark ignition engine, and the fuel containing 10% MTHF has comparable power outputs and CO, NO_x and HC emissions compared to unleaded gasoline [21]. The blend with a higher MTHF percentage (40%) could produce significant reductions in HC and benzene emissions and increases in NO_x [22]. Investigation of pollutants formation of MTHF in laminar premixed flames using molecular beam mass spectrometry (MBMS) and gas chromatograph (GC) revealed that ethylene is the largest production for MTHF, instead of acetylene or unsaturated furan family fuels [23].

The injection timing significantly affects fuel-air mixing procedure and the mixture quality in the combustion chamber. This also influences the combustion and emissions characteristics of the engine. In addition, the combustion stability, in DISI engine, is very sensitive to the fuel distribution near the spark plug [24,25]. The crank angle at which combustion starts is significantly influence by fuel injection timing. As the fuel injection timing varies the state of the air into which the fuel is injected also changes and this also varies the ignition delay. NO_x emissions for direct injection engines are strongly influence by fuel injection timing. NO_x emissions are commonly reduced by retarded injection timing. When the fuel injection timing is retarded, the combustion chamber temperatures dropped, thereby reducing NO_x by controlling spatial development of localized high temperature regions [26]. Although, many reports have investigated the combustion of low blends of MF and MTHF in gasoline, none has actually reported the HC speciation of MF20 and MTHF20 and the percentage of the unburned furan samples in the total organic compound emission of both MF20 and MTHF20.

In this study, the gaseous emissions characteristics of MF20 (MF 20% vol. and gasoline 80% vol.) and MTHF20 (MTHF 20% vol. and gasoline 80% vol.) were investigated in a single cylinder spray guided DISI engine using Gasmeth Fourier-Transform Infrared Spectroscopy (FTIR) as the emission measuring devise. Experiments were conducted at stoichiometric specific air–fuel ratio ($\lambda = 1$) and at constant engine speed of 1500 rpm using the fuels optimised spark timing. Effects of fuel injection sweeps (180–280 °CA BTDC**)** on the emission characteristics of the blends were investigated at the intermediate load of 5.5 bar IMEP. The HC speciation emissions including unburnt furan samples were studied for the three fuels investigated. The components of the HC emissions investigated in this study includes the unburn furan samples, ethylene, propene, benzene, ethanol, methane, acetylene, butane, octane, and acetic acid. The potential toxicity of furan-based fuels is a great restriction to its public acceptability as engine fuels. This is the first study that investigated the percentage of unburnt furan samples in the emission of MF20 and MTHF20. The conclusion indicated that the reported emission level of the unburnt furan fuel in the combustion of the blends fuel is very low and could be considered for safe human exposure. The FTIR use for this study, does not measure particle emissions. Particle matter is removed from the sample to ensure that representative samples of the flue gases were measured. The particle emissions was measured using digital multiplex system (DMS) 500.

2. Experimental System and Methods

2.1. Engine and Instrumentation

The engine specifications for the experiment on single-cylinder spray-guided DISI engine are listed in Table 1. The engine was naturally aspirated with a throttle controlling the intake air flow rate. In order to maintain a constant speed (±1 rpm), a direct current dynamometer was coupled to the engine. An in-house built software written in LabView was used for the engine timing. All temperatures were measured with a K-type thermocouple and all tests were conducted with coolant and lubricant oil temperatures maintained at 85 ± 2 °C and 90 ± 3 °C respectively and at the intake air temperature of 30 ± 2 °C. Figure 1, illustrates the schematic of the engine testing system. The fuel flow rate is calculated using the medusa engine specific parameter and engine operation parameter to be 0.124 g/s. There is an exhaust plenum chamber 8 times the swept volume of the cylinder located 15 cm downstream of the exhaust valves which is very common in many experimental single-cylinder engine setups. The exhaust plenum is used to stabilise the pressure fluctuation in the exhaust gas before getting to the Lambda meter to measure the air-fuel ratio.

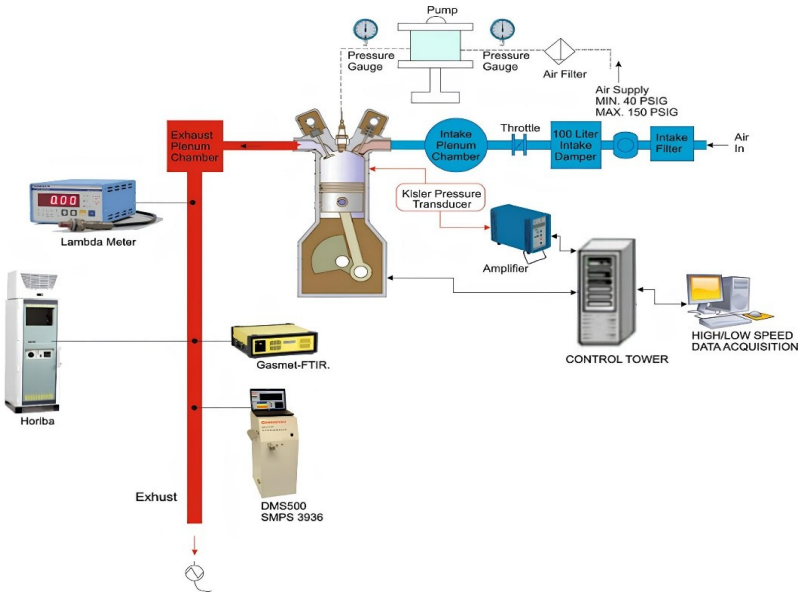

Figure 1. Engine testing system.

Table 1. Engine specifications.

Engine Type	4 Strokes, 4 Valve
Swept volume	565.6 (cm^3)
Bore	90 (mm)
Stroke	88.9 (mm)
Connecting rod length	160 (mm)
Compression ratio	11.5
Intake valve opening	16.5 (°CA BTDC *)
Exhaust valve closing	36.7 (°CA BTDC *)
Fueling type	Spray-guided DI

* TDC refers to the one in the gas exchange overlap.

In-cylinder pressure was measured by a water-cooled pressure transducer (Kistler 6041A) and combustion pressure data was recorded with the resolution of 0.2 crank angle degree (CAD). Gross Indicated mean effective pressure (IMEP) was calculated from the pressure data. The crankshaft encoder signal

determines the location of the piston relative to the top dead center (TDC) and is used by the Engine Timing Control Software (ETCS) to control the injection, ignition, and variable valve timing. During the experiments, all of the control signals are based on the 1440TTL pulses per cycle clock signals (2 pulse/CAD). FTIR technology by Gasmeth was used to measure the gaseous emissions. The FTIR complies with the requirements of US EPA Method 320-Vapour Phase organic and inorganic emissions by extractive FTIR [27]. Gaseous Emissions measured in this experiment include carbon monoxide (CO), Nitrogen oxide (NO), Nitrous oxide (N_2O), and the Total hydrocarbon species methane (CH_4), ethylene (C_2H_4), propene (C_3H_6), benzene (C_6H_6), ethanol (C_2H_6O), acetylene (C_2H_2), butane (C_4H_{10}), octane (C_8H_{18}), acetic acid (CH_3COOH), formaldehyde (CH_2O) and acetaldehyde (CH_3CHO). The FTIR monitors all the species continuously. The entire spectrum is scanned ten times per second and an average calculated from this is reported for each (user-selectable) sampling period. The Unburnt furan fuel in the emissions was identified in the FTIR analyser as an unknown species from the residual spectrum. The emission measurements were commenced after the engine was fully stabilised.

2.2. Test Fuels

The gasoline used in this study was supplied by Shell Global Solutions (UK). The neat MF and MTHF were supplied by Fisher Scientific, UK, with 99% purity level. Table 2 shows the properties of the base fuels. The test fuels are neat gasoline, MF20 (20% MF with 80% gasoline by volume), and MTHF20 (20% MTHF with 80% gasoline by volume).

Table 2. Base fuel properties [12,15,28,29].

Item	Gasoline	MF	MTHF
Chemical formula	C_6H_{14}–$C_{10}H_{22}$	C_5H_6O	$C_5H_{10}O$
Density (g/cm^3)	0.745	0.913	0.854
Research octane number (RON)	96.8	103	88.2
Motor octane number (MON)	85.7	86	71.2
Stoichiometric air/fuel ratio	14.46	10.05	11.16
Initial boiling point/Boiling point (°C)	32.8	64	80.3
Lower heating value (MJ/kg)	42.9	31.2	34.12
Lower heating value (MJ/L)	31.9	28.5	29.2
Heat of vaporization (kJ/kg)	373	358	375.3
Reid vapour pressure (kPa)	32.8	18.5	13.6
Oxygen mass fraction (%)	0.1	19.49	18.58
Solubility in water (vol. %)	Negligible	0.3	12.1

3. Result and Discussion

The engine-out emissions for the three fuels under investigations was measured with Gasmeth-FTIR. Regulated emissions of CO, NO_x and HC were studied. The components Percentage of the unburn furan sample species in the Hydrocarbon emissions were evaluated for both MF20 and MTHF20. CO_2 emissions and the unregulated emissions for the two blends fuels were measured and compared to that of the neat gasoline at the intermittent load of 5.5 bars IMEP. The effect of injection timing sweep on the particulate emission characteristics were discussed for each of the fuel investigated.

3.1. Gaseous Emissions Characteristics for the Combustion of the Fuels

Carbon monoxide emissions from internal combustion engine are controlled by the fuel/air equivalent ratio. For fuel-rich mixture, CO concentration in the exhaust increase steadily with increasing equivalent ratio, as the amount of excess fuel increases [30]. This trend is observed in Figure 2a. As the fuels injection timing retards the resulting mixture formation became poor which increases the amount of unburn fuel

leading to increased CO formations for the three fuels investigated. Formation of CO occurs when there is not enough oxygen present to produce CO_2. Advancing the fuels injection timing results in lean mixture and the resulting homogeneous mixture formations which leads to drastic reduction in CO emissions for the three fuels. By advancing the fuel injection timing to 280 CAD BTDC the CO emissions reduces by 36%, 50%, and 60% for the neat gasoline, MF20 and MTHF20 respectively. Gasoline shows lower CO emission compares to MF20 and MTHF20. The reason for this is because; the actual homogenous level for each of the three fuels in the combustion chamber is different due to their different inlet fuel film evaporation characteristics. Gasoline relatively forms combustible mixture easily due to its significant volatility. The combine effect of shorter injection timing and shorter fuel spray penetration which reduces the effect of piston crown wetting also explain why CO emission level of gasoline is lower than that of the two blend fuels. CO emission by MTHF20 is observed to be higher than MF20 because of the latter increase oxygenated content. Carbon monoxide is a product of incomplete combustion. More oxygen available in the molecular structure of MF20 leads to increase CO_2 emissions and thus the reason for reduction in its CO emission level compared to MTHF20.

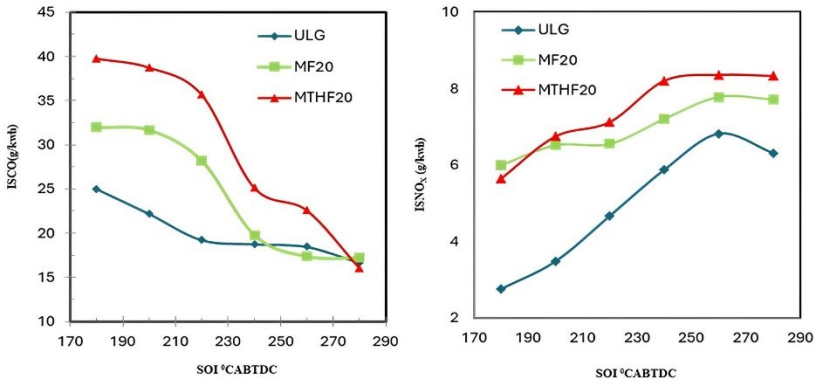

(**a**) (**b**)

Figure 2. (**a**) CO emissions and (**b**) NO_x emissions for un-leaded gasoline (ULG), MF20 and MTHF20 at 5.5 bar IMEP and at SOI of 180–280 °CA BTDC.

Chemical kinetic shows that the formation of NO and other oxides of nitrogen increases very strongly with increasing flame temperature [30]. Dissociation of diatomic nitrogen (N_2) to monatomic nitrogen (N) is highly influenced by higher combustion reaction temperature and the more monatomic nitrogen [N] formed the more NO_x (NO and NO_2 combined) will be produced. This trend is observed in Figure 2b, where NO_x emission for MF20 and MTHF20 are observed to be significantly higher than that of the neat gasoline across all the fuel injection timings because of their high in-cylinder peak flame temperatures. The oxygen contents of MF20 and MTHF20 are higher than that of the neat gasoline and addition of oxygen which corresponds to a reduction in diluent fraction increases flame temperatures and therefore NO_x emissions. All these explain the reason for the higher NO_x emission by the blend fuels compared to the neat gasoline. The time at which the fuel is injected into the combustion chamber significantly determine the crank angle at which the combustion commences. By retarding the fuel injection to 180 °CA BTDC, NO_x emissions were reduced by about 44%, 15% and 14% for the neat gasoline, MF20 and MTHF20 respectively. The reason for the NO_x lower emission at retarded fuel injection timing is because of the reduce combustion flame temperature in this region. However, the retarded timing could promote the increased formation of Nitrogen oxide (NO) in the exhaust formation due to insufficient timing for air fuel mixing at the late injection.

Figure 3 shows the trends of the fuel injection timing sweeps (180−280 ° CA BTDC with the instantaneous total hydrocarbon (isHC) emissions for MF20, MTHF20 and gasoline at the intermediate loads of 5.5 bar IMEP. It was observed that HC emissions decreases as the fuel injection timing advances for the three fuels investigated. Maximum emissions of the hydrocarbon were observed for the fuels at the late fuel injection of 180 °CA BTDC. Better fuel-air mixing is resulted when fuel is injected earlier in the compression

stroke which gives more time for the fuel to mix with the incoming air thereby allowing the fuel to burn more completely, resulting in reduced unburned hydrocarbons in the exhaust. Late fuel injection occurs later in the compression stroke, leading to less time for the fuel to mix adequately with the air before ignition. The result of which is incomplete combustion, resulting in higher HC emissions. Knocking is the spontaneous combustion of the air-fuel mixture due to high temperatures and pressures may result from late injection which can cause partially burned hydrocarbons to be expelled in the exhaust. Knocking can cause an increase in hydrocarbon emissions as well. HC emissions for oxygenated fuels are lower compared to gasoline. At the load of 5.5 bar IMEP and 280 °CA BTDC, both MF20 and MTHF20 display significant reduction in the HC of 34% and 11% respectively compared to the neat gasoline.

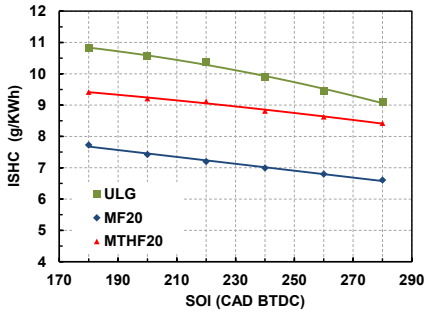

Figure 3. HC emission for ULG, MF20 and MTHF20 at 5.5 bar IMEP and at SOI of 180–280 °CA BTDC.

3.2. Hydrocarbon Emissions Speciation with Fuel Injection Timing

Figure 4 shows the percentage of the HC species for the three fuels at the intermediate loads of 5.5 bar IMEP and at the optimum fuel injection timing of 280 °CA BTDC. FTIR technology by Gasmeth was used to measure the gaseous emissions. The FTIR complies with the requirements of US EPA Method 320-Vapour Phase organic and inorganic emissions by extractive FTIR [31]. The FTIR monitors all the species continuously. The entire spectrum is scanned ten times per second and an average calculated from this is reported for each (user-selectable) sampling period. Species are measured individually and can be added together analytically. The unburned furan-based fuel was identified in the FTIR analyser as an unknown species from the residual spectrum. Generally, the HC species proportions of MF20 and MTHF20 are similar to that of gasoline; however, there are some differences in their percentage compositions. Ethylene, butane, propene, benzene, acetylene, octane, and ethanol constituted more than 90% of the total HC species for each of the fuels investigated. Gasoline has a higher proportion of octane, acetic acid, and methane than both MF20 and MTHF20. MF20 blend has higher proportion of acetylene and lower proportion of ethanol than gasoline and MTHF20. As indicated in Figure 4a–c; ethylene with components percentage of 25%, 26% for and 25% for Gasoline, MF20 and MTHF20 respectively, consistently remains the highest components of the isHC. Methane is a greenhouse gas, however, its percentage emissions in HC is very low for the three fuels. Ethylene is a greenhouse gas, and excessive emissions contribute to climate change and global warming. It can also react with other air pollutants to form ground-level ozone, which can harm plant life, reduce crop yields, and contribute to smog formation [32,33]. Exposure to high concentration of ethylene (thousands of parts per million) can cause dizziness, anesthesia, drowsiness, or other central nervous system effect [34,35]. Ethylene in the air in an enclosed placed will decrease the amount of oxygen present. Prolonged exposure to elevated levels of ethylene may lead to more severe respiratory issues and long-term health problems [36,37]. Propene is a volatile organic compound (VOC) and is considered a precursor to ground-level ozone formation, which contributes to the formation of smog [37, 38]. According to the results as indicated in Figure 4b,c, percentage of the unburn furan in the combustions of MF20 and MTHF20 was observed to be around 3% of the HC. This percentage of unburn furan could be considered safe for human exposure, but further investigation is required in this field. Figure 5a–c shows the variation of the Hydrocarbon emissions species with the fuel injection timing. The result indicated that the emissions of all the hydrocarbon species except propene reduces as fuel injection advances toward 280 °CA BTDC. When the fuel injection timing is advanced, it means that the fuel is injected into the engine's cylinder earlier in the compression stroke. This

can cause the fuel-air mixture to ignite too early in the compression stroke. As a result, the combustion process may not be completed fully before the exhaust valve opens. Incomplete combustion leads to the production of higher levels of unburnt hydrocarbons.

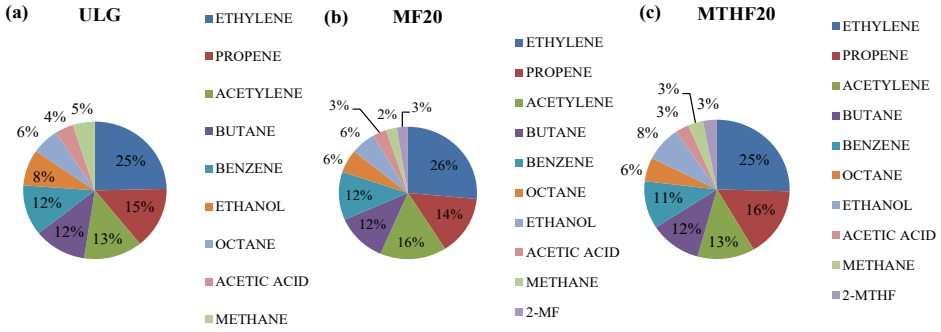

Figure 4. HC speciation for (**a**) ULG, (**b**) MF20, and (**c**) MTHF20 at 5.5 bar IMEP and 280 °CA BTDC.

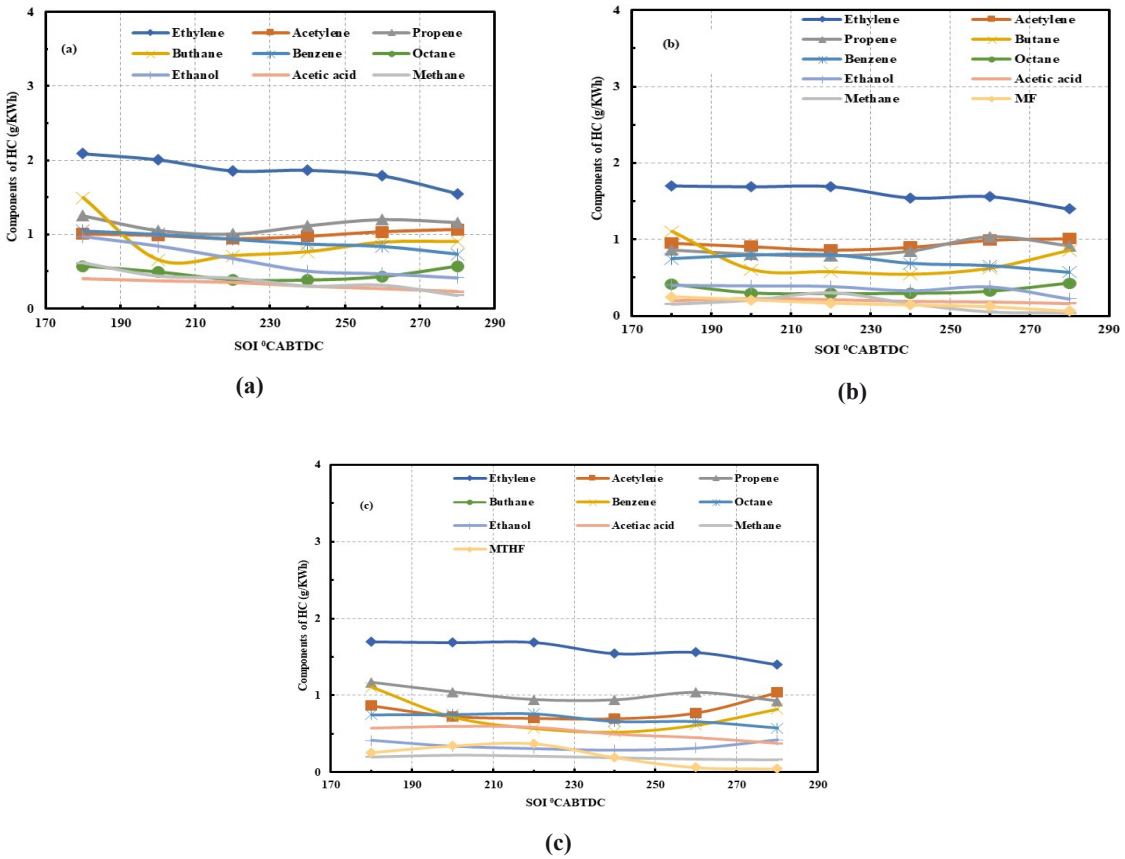

Figure 5. (**a**) HC speciation for ULG at 5.5 bar IMEP and SOI of 180–280 °CA BTDC; (**b**)HC speciation for MF at 5.5 bar IMEP and SOI of 180–280 °CA BTDC; (**c**) HC speciation for MTHF at 5.5 bar IMEP and SOI of 180–280 °CA BTDC.

3.3. Unburnt Furan Component of the Hydrocarbon Emissions

The variations of the percentage of the unburnt furan fuel in the hydrocarbon emissions with fuel injection timing are recorded in Figure 6. Although both MTHF20 and MF20 have their percentage emission of unburnt furan as 3% of the total hydrocarbon at the optimum injection timing, the unburnt furan emission

at the late fuel injection was significantly higher for MTHF20 than that of MF20 by about 80%, these values reduce significantly with the advance in fuel injection timing and at the optimum timing of 280 °CA BTDC. the unburnt furan emissions for the two-blend fuel have reduce significantly by 87.5% and 33.3% for MTHF20 and MF20 respectively from the value recorded at 220 °CA BTDC. The danger of unregulated human exposure to furan includes, respiratory distress, increased secretory response, and death [39,40] and liver and kidneys and to a lesser extent lungs and intestines infections [41].

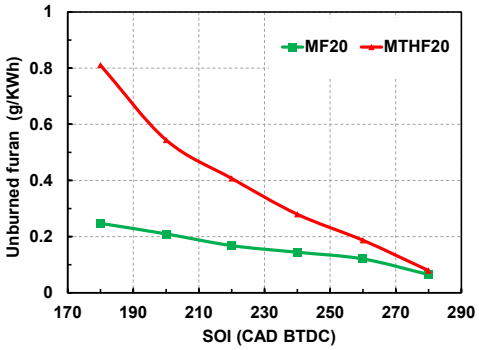

Figure 6. Unburn furan samples in MF20 and MTHF20 at 5.5 bar IMEP and at SOI of (180–280 °CA BTDC).

Based on a chronic oral carcinogenicity study in which clear evidence of carcinogenicity was noted in male and female rats and mice, the National Toxicology Program (NTP) classifies furan as "reasonably anticipated to be a human carcinogen" and the International Agency for Research on Cancer (IARC) lists furan as a Group 2B carcinogen (possibly carcinogenic to humans). This finding revealed that the percentage of unburnt furan emission in engine combustion is low to be considered save for human exposure. However, it is established in Figure 6 that percentage of the unburned furan emissions reduces as the fuel injection timing advances.

3.4. Acetaldehyde and Formaldehyde

The two unregulated emission measured in this study are the acetaldehyde (CH_3CHO) and formaldehyde (CH_2O) emissions. Although, unregulated emissions are not limited to these two, but formaldehyde and acetaldehyde constitutes about 70% of this group. The emissions of formaldehyde and acetaldehyde for the two blends fuels (MF20 and MTHF20) was consistently lower than that of the neat gasoline across the fuel injection sweep as indicated in Figures 7 and 8 respectively. At early fuel injection timing of 280 °CA BTDC. there was significant increase in the level of emissions of both formaldehyde and acetaldehyde for the three fuels. The emissions of the two unregulated compounds thereafter remain constant as the fuel injection timing retards from 220 °CA BTDC. to 180 °CA BTDC. This trend is true for all the three fuels investigated. The observed trends of emissions of the two unregulated compounds are similar to that of the hydrocarbon emissions influenced by the fuel oxygenation contents.

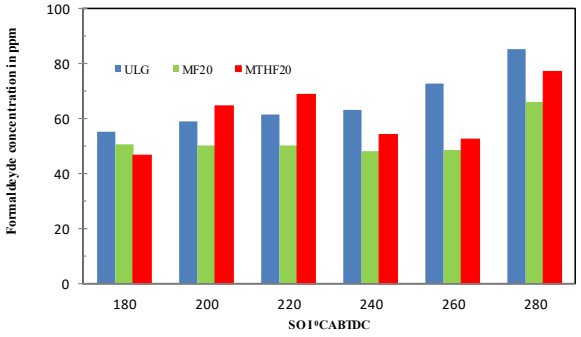

Figure 7. Formaldehyde emissions for ULG, MF20 and MTHF20 at SOI of (180–280 °CA BTDC).

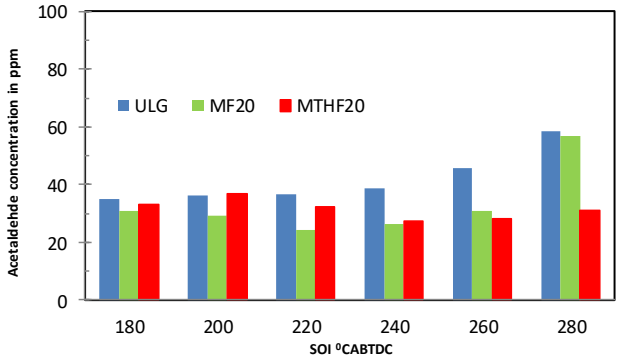

Figure 8. Acetaldehyde emissions for ULG, MF20 and MTHF20 at SOI of (180–280 °CA BTDC).

3.5. CO_2 Emissions

Carbon dioxide (CO_2) emission is not a legislated combustion product but is one of the substances responsible for global temperature rises through the greenhouse effect. The Figure 9 shows the CO_2 emissions for ULG, MF20 and MTHF20 at SOI (180–280 °CA BTDC). Results indicates that the CO_2 emissions of MF20 and MTHF20 is a little less than that of the gasoline because of their higher energy density which reduces the rate of fuel consumed compares to gasoline. At the late injection timing of 180 °CA BTDC, the higher percentage of CO_2 emissions was due to the increase CO molecules resulting from incomplete combustion created by poor mixture formation in this region. As the fuel injection timing advances and the resulting mixture formation become lean and significant drop in the percentage of CO_2 emission was observed. This is due to the fact that in this region the mixture formation tends to become homogeneous and less CO gaseous molecules were produced which ultimately lead to the reduction in the level of CO_2 emissions.

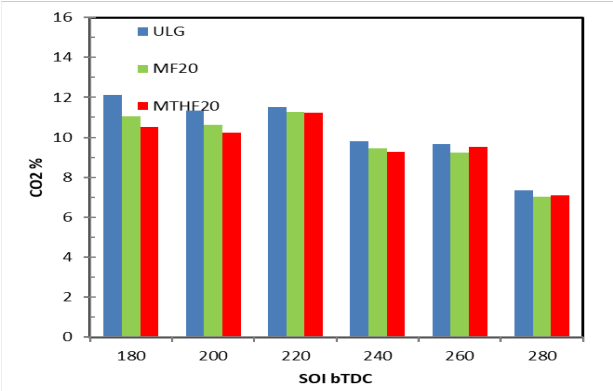

Figure 9. CO_2 emissions for ULG, MF20 and MTHF20 at SOI (180–280 °CA BTDC).

3.6. Particulate Emissions for Gasoline and the Blend Fuels

Particulate matter (PM) size distribution basically consists of two modes [42] the nucleation mode and the accumulation mode. The nucleation mode has more influence in number of particles while the accumulation mode is concern with the particle mass distribution due to its higher size. The PM size distributions for MTHF20, MF20 and gasoline. at 5.5 bar IMEP are shown in Figure 10. For both MTHF20, MF20 and gasoline, there are overlaps between nucleation mode and accumulation mode. Many researchers have used diameter range to separate nucleation and accumulation modes. Kittel son suggested: 0–50 nm for nucleation mode and 50–1000 nm for accumulation mode [43, 44]. Eastwood suggested: 0–100 nm for nucleation mode and 100–900 nm for accumulation mode [45].

In this study, the MATLAB script developed by University of Castilla-La Mancha was used to differentiate the two modes. Fuel properties such as the oxygen contents of the fuels have direct impact on the PM emissions. High oxygenated fuels tend to produce less soot. The soot level can dramatically affect the

shape of the particle size distribution. Higher soot emissions increase the chance of gaseous HC adsorption and condensation on its surface forming wet coating, reducing the available hydrocarbons for nucleation. The detailed summary of PM emissions data are shown in the Table 3.

Table 3. Summary of PM emissions for gasoline, MF20 and MTHF20.

	Nucleation Mode			Accumulation Mode		
	ULG	**MF20**	**MTHF20**	**ULG**	**MF20**	**MTHF20**
Number (#/cm^3)	4.63×10^9	3.43×10^9	4.22×10^9	1.14×10^8	2.59×10^7	6.31×10^7
Mass(μg/cm^3)	0.0085	0.0068	0.0066	0.1229	0.0136	0.0557

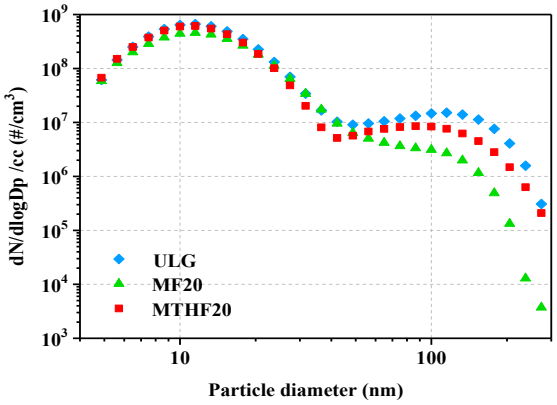

Figure 10. Peak PM emissions for ULG, MF20, and MTHF20 at 5.5 bar IMEP and 280 °CA BTDC.

Hydrocarbons are adsorbed or condensed on soot particles, which increase the size and increase the chance for wet soot to collide with each other and form even bigger soot particles. Higher HC emissions tend to increase the total number of particles and increase the mean diameter for both nucleation and accumulation mode. From Figure 10, at 5.5 bar IMEP, MF20 has the lower PM emissions than that of gasoline and MTHF20. The higher oxygen content in MF20 molecule and lower HC emissions compared to gasoline and MTHF20 can be used to explain why MF20 has smaller mean diameter.

4. Conclusions

The FTIR used for this study provided the unique opportunity to measure the components of the hydrocarbon emissions. along with the regulated and unregulated emissions for the three fuels investigated. Based on the experimental result, the following conclusion were drawn.

- Retarding the fuel injection timing reduces the NO_x emission for the three-fuel investigated. This is due to the reduce combustion flame temperature in this region at the retarded SOI timing.
- The HC emissions decreases as the fuel injection timing advances for the three fuels investigated. At the load of 5.5bar IMEP and 280 °CA BTDC, both MF20 and MTHF20 display significant reduction in the HC of 34% and 11% respectively compared to the neat gasoline.
- Higher CO emission was noticed for the three fuels as injection timing retards because of the poor fuel mixture formation and the effect of rich mixture at this timing. However, un-leaded gasoline (ULG) emits low CO compared to MF20 and MTHF20 because of its significant volatility, high energy density and shorter fuel spray penetration.
- The highest components of the total hydrocarbon emissions is the Ethylene samples with percentage emissions of 25–26% of the total organic compound emissions.
- The result indicated that the emissions of all the hydrocarbon species except propene reduces as fuel injection advances toward 280 °CA BTDC.
- It is established in figure8 that percentage of the unburned furan emissions reduces as the fuel

injection timing advances. And the percentage of unburnt furan emission of MF20 and MTHF20 is about 3% of the total hydrocarbon emission. This percentage emission of the unburned furan components in HC is low and could considered safe for human exposure.

5. Future Work

The actual safe human exposure level to the engine combustion of furan based fuels needs to be experimentally determined in order to establish its safety to human health as engine fuels and to justify further huge investment into furan fuels researches as alternative fuels to ethanol and gasoline.

Nomenclature

BTDC	before top dead center
CO	carbon monoxide
CO_2	carbon dioxide
°CA	crack angle degree
DISI	direct-injection spark ignition
DOE	Department of Energy
DMF	2,5-dimethyl-furan
EGR	exhaust gas recirculation
FID	flame ionization detector
FTIR	Fourier-transform infrared spectroscopy
GC	gas chromatograph
HC	hydrocarbon
IMEP	indicated mean effective pressure
MF	2-methylfuran
MTHF	2-methyltetrahydrofuran-
MBT	maximum brake torque
MBMS	molecular beam mass spectrometry
MON	motor octane number
NO_x	nitrogen oxides
RON	research octane number
SI	spark ignition
ULG	un-leaded gasoline

Author Contributions: Conceptualization, R.O.; methodology, R.O.; validation, R.O., G.Z. and H.X.; formal analysis, R. O. and G. Z.; investigation, R. O. and G. Z.; resources, R. O.; data curation, R. O. and G. Z.; writing—original draft preparation, R.O.; writing—review and editing, R.O., G.Z. and H.X.; visualization, R.O. and G.Z.; supervision, H.X.; project administration, H.X.; funding acquisition, H.X. All authors have read and agreed to the published version of the manuscript.

Funding: This research received no external funding.

Data Availability Statement: Not applicable.

Acknowledgments: This work was conducted in the Future Engines and Fuels Laboratory at the University of Birmingham, UK. The authors thank Quantitech for making it possible to use the Gasmeth-FTIR for this research study, UK Shell Global solutions for the gasoline and Jaguar Motors for the DISI Engine and Lagos state University of Science and Technology and Tetfund Nigeria for the scholarship support.

Conflicts of Interest: The authors declare no conflict of interest.

References

1. Wei, H.; Feng, D.; Shu, G.; Pan, M.; Guo, Y.; Gao, D.; Li, W. Experimental investigation on the combustion and emissions characteristics of 2-methylfuran gasoline blend fuel in spark-ignition engine. *Appl. Energy* **2014**, *132*, 317–324.
2. Román-Leshkov, Y.; Barrett, C. J.; Liu, Z. Y.; Dumesic, J. A. Production of dimethylfuran for liquid fuels from biomass-derived carbohydrates. *Nature* **2007**, *447*, 982–985.
3. He, J.; Qiang, Q.; Liu, S.; Song, K.; Zhou, X.; Guo, J.; Zhang, B.; Li, C. Upgrading of biomass-derived furanic compounds into high-quality fuels involving aldol condensation strategy. *Fuel* **2021**, 306, 121765.
4. Zhao, H.; Holladay, J. E.; Brown, H.; Zhang, Z. C. Metal chlorides in ionic liquid solvents convert sugars to 5-hydroxymethylfurfural. *Science* **2007**, *316*, 1597–1600.
5. Dumesic, J. A.; Roman-Leshkov, Y.; Chheda, J. N. Catalytic Process for Producing Furan Derivatives from Carbohydrates in a Biphasic Reactor. Google Patents No. 2653706A; 12 May 2015.
6. Eldeeb, M. A.; Akih-Kumgeh, B. Recent trends in the production, combustion and modeling of furan-based fuels. *Energies* **2018**, *11*, 512.
7. Liu, H.; Olalere, R.; Wang, C.; Ma, X.; Xu, H. Combustion characteristics and engine performance of 2-methylfuran compared to gasoline and ethanol in a direct injection spark ignition engine. *Fuel* **2021**, 299, 120825.
8. Wang, X.; Gao, J.; Chen, Z.; Chen, H.; Zhao, Y.; Huang, Y.; Chen, Z. Evaluation of hydrous ethanol as a fuel for internal combustion engines: A review. *Renewable Energy* **2022**, *194*, 504–525.
9. Zhou, Z.; Yan, F.; Zhang, G.; Wu, D.; Xu, H. A Study on the Dynamic Collision Behaviors of a Hydrous Ethanol Droplet on a Heated Surface. *Processes* **2023**, *11*, 1804.
10. Jin, C.; Geng, Z.; Liu, X.; Ampah, J. D.; Ji, J.; Wang, G.; Niu, K.; Hu, N.; Liu, H. Effects of water content on the solubility between Isopropanol-Butanol-Ethanol (IBE) and diesel fuel under various ambient temperatures. *Fuel* **2021**, *286*, 119492.
11. Qian, Y.; Zhu, L.; Wang, Y.; Lu, X. Recent progress in the development of biofuel 2, *5*-dimethylfuran. *Renewable Sustainable Energy Rev.* **2015**, *41*, 633–646.
12. Van, V.; Stahl, W.; Nguyen, H.V.L. The heavy atom microwave structure of 2-methyltetrahydrofuran. *J. Mol. Struct.* **2016**, *1123*, 24–29.
13. Ma, X.; Jiang, C.; Xu, H.; Ding, H.; Shuai S. Laminar burning characteristics of 2-methylfuran and isooctane blend fuels. *Fuel* **2014**, *116*, 281–291.
14. Pan, M.; Shu, G.; Pan, J.; Wei, H.; Feng, D.; Guo, Y.; Liang, Y. Performance comparison of 2-methylfuran and gasoline on a spark-ignition engine with cooled exhaust gas recirculation. *Fuel* **2014**, *132*, 36–43.
15. Wang, C.; Xu, H.; Daniel, R.; Ghafourian, A.; Herreros, J. M.; Shuai, S.; Ma, X. Combustion characteristics and emissions of 2-methylfuran compared to *2*, 5-dimethylfuran, gasoline and ethanol in a DISI engine. *Fuel* **2013**, *103*, 200–211.
16. Hoang, A.T. 2-Methylfuran (MF) as a potential biofuel: A thorough review on the production pathway from biomass, combustion progress, and application in engines. *Renewable Sustainable Energy Rev.* **2021**, *148*, 111265.
17. Parry, L. Engine Combustion and Emission Performance of Furan Fuels in Comparison to Conventional Automotive Fuels. Ph.D. Thesis, University of Birmingham, Birmingham, UK, 2020.
18. Thewes, M.; Muether, M.; Pischinger, S.; Budde, M.; Brunn, A.; Sehr, A.; Adomeit, P.; Klankermayer, J. Analysis of the impact of 2-methylfuran on mixture formation and combustion in a direct-injection spark-ignition engine. *Energy Fuels* **2011**, *25*, 5549–5561.
19. Canakci, M.; Ozsezen, A. N.; Alptekin, E.; Eyidogan, M. Impact of alcohol—Gasoline fuel blends on the exhaust emission of an SI engine. *Renewable Energy* **2013**, *52*, 111–117.
20. Bluhm, K.; Heger, S.; Redelstein, R.; Brendt, J.; Anders, N.; Mayer, P.; Schaeffer, A.; Hollert, H. Genotoxicity of three biofuel candidates compared to reference fuels. *Environ. Toxicol. Pharmacol.* **2018**, *64*, 131–138.
21. Talibi, M.; Hellier, P.; Ladommatos, N. Investigating the Combustion and Emissions Characteristics of Biomass-Derived Platform Fuels as Gasoline Extenders in a Single Cylinder Spark-Ignition Engine. In *SAE Technical Papers*; SAE International: Warrendale, PA, USA, 2017.
22. Rudolph, T.; Thomas, J. NO_x, NMHC and CO emissions from biomass derived gasoline extenders. *Biomass* **1988**, *16*, 33–49.
23. Tran, L.-S.; Glaude, P.-A.; Battin-Leclerc, F. Experimental study of pollutants formation in laminar premixed flames of tetrahydrofuran family fuels. In Proceedings of the 8th US National Combustion Meeting, Salt Lake City, UT, USA, 19–22 May 2013; pp. 1–15.
24. Abraham, J.; Bracco, F.; Reitz, R. Comparisons of computed and measured premixed charge engine combustion. *Combust. Flame* **1985**, *60*, 309–322.
25. Jayashankara, B.; Ganesan, V. Effect of fuel injection timing and intake pressure on the performance of a DI diesel engine–A parametric study using CFD. *Energy Convers. Manage.* **2010**, *51*, 1835–1848.
26. Suryawanshi, J.G.; Deshpande, N. Effect of injection timing retard on emissions and performance of a pongamia oil methyl ester fuelled CI engine. In *SAE Technical Paper*; SAE International: Warrendale, PA, USA, 2005.
27. Austin, E.; Hoang, K.T. Evaluation of gasmet TM DX-4015 series Fourier transform infrared gas analyzer. In *DTIC Document*; DTIC: Fairfax, VA, USA, 2009.
28. Daniel, R.; Tian, G.; Xu, H.; Wyszynski, M.L.; Wu, X.; Huang, Z. Effect of spark timing and load on a DISI engine fuelled with 2, *5*-dimethylfuran. *Fuel* **2011**, *90*, 449–458.

29. Lucas, S.V.; Loehr, D.A.; Meyer, M.E.; Thomas, J.; Gordon, E.E. Exhaust emissions and field trial results of a new, oxygenated, non-petroleum-based, waste-derived gasoline blending component: 2-methyltetrahydrofuran. In *SAE Technical Paper*; SAE International: Warrendale, PA, USA, 1993.
30. Heywood, J.B. *Internal Combustion Engine Fundamentals;* McGraw-Hill Education: New York, NY, USA, 2018.
31. Madsen, J.; Bjerg, B.S.; Hvelplund, T.; Weisbjerg, M.R.; Lund, P. Methane and carbon dioxide ratio in excreted air for quantification of the methane production from ruminants. *Livest. Sci.* **2010**, *129*, 223–227.
32. Gupta, S.K.; Da, Y.; Zhang, Y.-B.; Pandey, V.; Zhang, J.-L. Tropospheric ozone is a catastrophe, and ethylenediurea (EDU) is a phytoprotectant, recent reports on climate change scenario: A review. *Atmos. Pollut. Res.* **2023**, *14*, 101907.
33. Ainsworth, E.A. Understanding and improving global crop response to ozone pollution. *Plant J.* **2017**, *90*, 886–97.
34. Levin, S.; Lilis, R. Diseases Associated with Exposure to Chemical Substances. *Public Health Preventive Med.* **2008**, 619.
35. van Thriel, C.; Boyes, W.K. Neurotoxicity of organic solvents: An update on mechanisms and effects. In *Advances in Neurotoxicology*; Elsevier: Amsterdam, Netherlands, 2022; pp. 133–201.
36. Keller, N.; Ducamp, M.N.; Robert, D.; Keller, V. Ethylene removal and fresh product storage: A challenge at the frontiers of chemistry. Toward an approach by photocatalytic oxidation. *Chem. Rev.* **2013**, *113*, 5029–5070.
37. Yang, X.; Gao, L.; Zhao, S.; Pan, G.; Fan, G.; Xia, Z.; Sun, X.; Xu, H.; Chen, Y.; Jin, X. Volatile Organic Compounds in the North China Plain: Characteristics, Sources, and Effects on Ozone Formation. *Atmosphere* **2023**, *14*, 318.
38. Zhang, K.; Li, L.; Huang, L.; Wang, Y.; Huo, J.; Duan, Y.; Wang, Y.; Fu, Q. The impact of volatile organic compounds on ozone formation in the suburban area of Shanghai. *Atmos. Environ.* **2020**, *232*, 117511.
39. Terrill, J.; Van Horn, W.; Robinson, D.; Thomas, D. Acute inhalation toxicity of furan, 2-methylfuran, alcoholfurfuryl, and furfural in the rat. *Am. Ind. Hyg. Assoc. J.* **1989**, *50*, A359–A361.
40. Tabaran, A.F.; O'Sullivan, M.G.; Seabloom, D.E.; Vevang, K.R.; Smith, W.E.; Wiedmann, T.S.; Peterson, L.A. Inhaled Furan Selectively Damages Club Cells in Lungs of A/J Mice. *Toxicol. Pathol.* **2019**, *47*, 842–850.
41. EFSA Panel on Contaminants in the Food Chain; Knutsen, H.K.; Alexander, J.; Barregård, L.; Bignami, M.; Brüschweiler, B.; Ceccatelli, S.; Cottrill, B.; Dinovi, M.; Edler, L.; et al. Risks for public health related to the presence of furan and methylfurans in food. *EFSA J.* **2017**, *15*, e05005.
42. Eastwood, P. *Particulate Emissions from Vehicles*; John Wiley & Sons: Hoboken, NJ, USA, 2008.
43. Ursem, B. Climate shifts and the role of nano structured particles in the atmosphere. *Atmos. Clim. Sci.* **2015**, *6*, 51–76.
44. Kittelson, D.B. Engines and nanoparticles: A review. *J. Aerosol Sci.* **1998**, *29*, 575–588.
45. Armas, O.; Gómez, A.; Mata, C. Methodology for measurement of diesel particle size distributions from a city bus working in real traffic conditions. *Meas. Sci. Technol.* **2011**, *22*, 105404.